Ignition and Sustainment of Arcing on Nanostructured Tungsten under Plasma Exposure

Dogyun Hwangbo, Daisuke Nishijima, Shin Kajita, Russell P. Doerner, Sergey A. Barengolts, Mikhail M. Tsventoukh, Hirohiko Tanaka, and Noriyasu Ohno

***Abstract*—Laser-induced arc was initiated on a nanostructured 'fuzz' tungsten cathode with simultaneous exposure to a stationary helium (He) plasma. Arc spots moved randomly and eroded almost all the surface area. The diameter of each arc spot was measured to be 5-10 μm. A linear relationship was observed in the arc current-voltage characteristic, which was affected by the presence of resistance through a He plasma column. The specific resistance of He plasmas was estimated from the current-voltage characteristic, which showed a good agreement with theoretical calculations. A greater potential gap should be maintained to keep a higher arc current, indicating a good sign for preventing a high current arc in fusion devices. The condition of arc ignition was investigated in detail, by changing the He plasma parameters and the sheath potential drop. The ignition and sustainment of arcs were very sensitive to both the sheath potential drop and the sheath electric field. Arcs ignited when the sheath potential drop was negatively deeper than -100 V and the sheath electric field was above 2 MV/m. The relatively low electric field threshold would result from the thermo-field emission aided by heating of spots from adjacent former spots. This result indicates that the electron density and the electron temperature should be reduced in order to lower the potential drop and the sheath electric field in front of the plasma-facing material surface, which can prevent arcs from igniting in fusion devices.**

***Index Terms*—tungsten, divertor, nanostructure, unipolar arcing, nuclear fusion.**

I. Introduction

IN A THERMONUCLEAR fusion reactor, the dissipation of a heat load to plasma-facing components (PFCs) has been one of the most important issues. For instance, the heat load of 10 MWm^{-2} will be introduced to the ITER divertor target in the steady state of the standard operation campaign [1]. In addition, high energy transient events, such as edge localized modes (ELMs) will also be accompanied [1]. Therefore, as the divertor target material, tungsten (W) has been selected to tolerate the heat load, owing to its good refractory properties, such as high melting point, high thermal diffusivity and low physical sputtering yield as well as low fuel hydrogen retention compared to other candidate materials.

Besides fuel hydrogen isotopes, helium (He) ions are generated as a by-product of the fusion reaction and included in the ion fluxes. It has been known that He ions interact with W, forming various surface morphology changes. Especially, the nanostructuring of W, so-called 'fuzz' formation, occurs on a W surface, interacting with He plasmas [2], [3]. The formation condition for the fuzz growth has been clarified: the incident ion energy greater than 20 eV and the W temperature window of $1000-2000$ K are required for the fuzz growth [4]. Thus far, it is still under argument whether the fuzzy layer can be formed in future fusion devices. However, an estimation supports a possibility for fuzz to grow on the ITER divertor target, where the surface temperature and incident ion energy during the steady state operation would meet the formation condition for fuzz growth [1], [5], [6]. The W nanostructuring not only results in mechanical brittleness, but also induces considerable changes in thermal and electrical properties. Especially, the thermal diffusivity decrease [7] and an increase in the field electron emission property [8] strongly enhance an arc ignition possibility on the W fuzzy surfaces.

Unipolar arc ignition on PFCs has been a potential threat in fusion reactors, because it can induce bursty wall erosion and thus produce a large quantity of macro-particles, consequently leading to cooling down of core plasma and shortening of reactor lifespan. W can induce especially severe cooling down once macro-particles are released because of its property of being an high-Z material. Recently, arc ignitions have been reported in several large-scale experimental devices such as DIII-D [9], JT-60 [10], LHD [11], and ASDEX-U [12]. Especially, W-fuzz significantly eased the arc ignition owing to its drastic changes in thermal and electrical properties compared to a smooth W [13]. Since the first laboratory experiment of self-sustaining unipolar arcing was conducted using a fuzzy W target [14], the W-fuzz has further activated relevant researches: a voltage drop during the arc ignition [15] and a linear current-voltage characteristic which was mediated via a plasma column surrounding the target [16]. Regarding the arc ignition condition, the minimal target potential drop between a target and a surrounding plasma was revealed by several researches, which ranged at $60-100$ V [13], [15], [17]. However, the role of surrounding plasmas contributing to the arc ignition has not been clarified even though it is believed that the unipolar arc is maintained by interactions with the

D. Hwangbo, H. Tanaka and N. Ohno are with the Graduate School of Electrical Engineering, Nagoya University, Nagoya, 4648603 Japan. e-mail: hwangbo@nagoya-u.jp

D. Nishijima and R. P. Doerner are with Center for Energy Research, University of California San Diego, La Jolla, CA 92093, USA.

S. Kajita is with Institute of Materials and Systems for Sustainability, Nagoya University, 4648603 Japan.

S. A. Barengolts is with the Prokhorov General Physics Institute, Russian Academy of Sciences, Moscow 119991, Russia, and also with the Lebedev Physical Institute, Russian Academy of Sciences, Moscow 119991, Russia.

M. M. Tsventoukh is with the Lebedev Physical Institute, Russian Academy of Sciences, Moscow 119991, Russia

This work was supported by JSPS KAKENHI 15H04229, 17J05670 and JSPS Bilateral Joint Research Projects. This work was supported in part by LGS frontier program of Nagoya University by JSPS. This work was supported in part by the U.S. Department of Energy Grant No. DE-FG02-07ER54912. This work was supported in part by RFBR Grants 18-58-50005, 16-08-01306 and by the RAS Presidium (basic research programme I.11P).

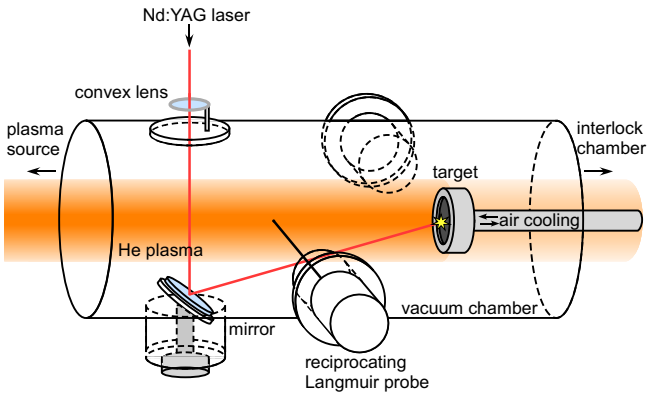

Fig. 1. A schematic of experiments. DC arc helium plasma is maintained throughout the experiment and a sample is biased negatively using a DC power supply to obtain an intended incident helium ion energy to make fuzz structure. A laser pulse is introduced on a fuzz surface to initiate arcing.

surrounding plasmas. Therefore, investigation on the effect of surrounding plasmas on the ignition and sustainment of arcing on W-fuzz is important.

In this research, the arc ignition condition is explored by changing the sheath potential drop and the sheath electric field, which are formed between the target surface and the surrounding plasma. Arc spots and their motion are observed using a scanning electron microscope. Arc current-voltage characteristics are analyzed, focusing on the effect of plasma resistance through a He plasma column.

II. Experimental Methods

A. Preparation of sample

The plasma irradiation and fabrication of nanostructured fuzzy layer on W samples was conducted in the linear divertor simulator PISCES-A [18]. It can produce a steady state high density plasma using a LaB_6 cathode heated by a tungsten heater. Fig. 1 shows a schematic of the experiment. A W target of 25 mm in diameter was sanded to remove any surface absorbates using a sand paper with a grit of 240 prior to plasma exposure, then installed to a target holder. The W target was biased negatively using a power supply (SORENSEN SGI 300/33, AMETEK) to control the incident ion energy to fulfill the fuzz formation condition. Fig. 2 shows images of sample surfaces. An example of sanded surfaces can be seen in Fig. 2(a). The area where the plasma irradiated was 22 mm in diameter. The surface temperature was measured by a thermocouple touching the backside of the sample and controlled via air cooling system as shown in Fig. 1. The plasma irradiation was conducted for 30 min. During the fabrication of fuzzy layer, the incident ion energy and the sample temperature were maintained at 100 eV and $\sim$1080 K, respectively. Typical electron temperature and density were measured using a reciprocating Langmuir probe and were $\sim$6 eV and $\sim 5 \times 10^{18}$ m^{-3}, respectively. The ion flux was $\sim 4 \times 10^{22}$ $m^{-2}s^{-1}$ and resultant ion fluence was $\sim 7 \times 10^{25}$ m^{-2}. These conditions give us an approximate fuzzy layer thickness of ~ 1 μm [19].

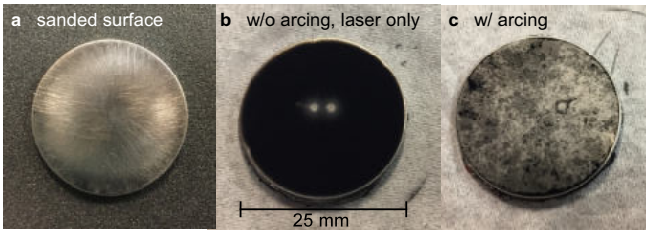

Fig. 2. Surface images of samples. (a) shows a sample surface which was sanded with a grit of 240. (b) shows a surface covered by fuzzy layer on which two pulsed laser spots remained. (c) shows a surface which was eroded by arc trails after the arc ignition.

B. Arc ignition

Arcing is sustained by the interactions between a negatively biased sample and existing stationary helium plasma. A laser pulse is used to produce an initial dense W plasma for arc initiation. After the fuzz growth, the surface became totally black as shown in Fig. 2(b). The first harmonic of an Nd:YAG laser pulse (1064 nm and 6 ns) was introduced on the fuzzy sample surface. The spot size of the laser was measured to have a diameter of $\sim$0.8 mm. The laser power was measured to be 2.7×10^{13} Wm^{-2}, which was sufficiently greater than the power requiring for the crater formation of 0.9×10^{11} Wm^{-2} on a smooth W surface [20]. The laser power also exceeded the threshold of 2×10^{12} Wm^{-2} for explosive-electron emission pulse at a clean surface [21]. When an arc occurred, the changes in current and voltage were recorded by an oscilloscope (Tektronix TBS1104). The current was measured using a current probe (Pearson current monitor model 3972). The rise time of the current probe (20 ns) was fast enough compared to the time resolution of the oscilloscope and the duration of arc signals. The voltage was measured via a BNC cable directly connected to the output of the power supply. Note that the current limit was set to 20 A for the power supply. To investigate the effect of surrounding He plasma on the arcing ignition in detail, we controlled the sheath potential drop between the target surface and the surrounding plasma, and He plasma discharge current which would change the He plasma parameters. Note that the surface temperature at which the arcs ignited was different for each sample and spread in the range of 680$-$1240 K, because the surface temperature greatly depends on the ion flux and the incident ion energy bombarding the target. After the arc ignition, most of the surface was eroded by arc spots, and fuzzy layer barely remained as an undamaged black surface, as shown in Fig. 2(c). For further detailing of the arc trails, the surface was observed using scanning electron microscopy (SEM).

III. Results and Discussion

A. Arc initiation

It is considered that arc ignition on a fuzzy surface follows two steps: first, dense plasma production by prompt laser heat load and, second, dense W-plasma action on the remaining fuzz nanowire layers that induce a strong electron emission into the W plasma, reaching an explosive level [22].

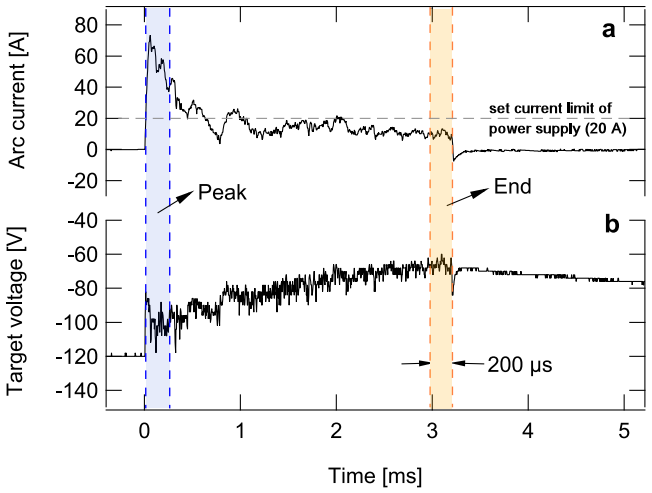

Fig. 3. Typical time evolution of (a) arc current and (b) target voltage when an arc ignited. Due to the slow rise time of the power supply, arc current typically exceeds the current limit (20 A) then gradually decreases. Values of voltage and current at the initial and the last 200 μs are cropped and used in Fig. 6. A mean current throughout an arc discharge is used in Fig. 4. For example, the peak current (I_{peak}), the end current (I_{end}) and the mean current (I_{avr}) shown above are 52.3, 8.6 and 15.6 A, respsectively.

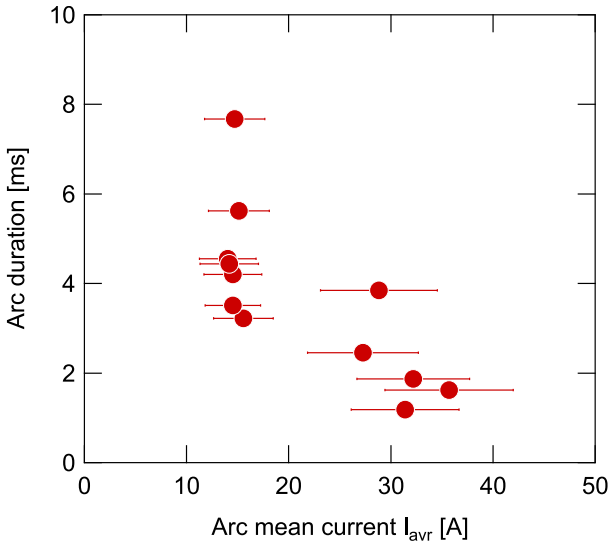

Fig. 4. The duration of arcs with respect to the arc mean current.

After the arc ignition, a majority of the sample surface was eroded, as typically shown in Fig. 2(c). Fig. 3 shows the typical time evolution of arc current and corresponding target voltage. An arc was initiated by introducing a laser pulse and sustained for several ms even after the laser irradiation. The arc current suddenly increased and peaked right after the initiation, then slowly decreased to 20 A or lower, the current limit for the power supply. Correspondingly the target voltage also changed gradually. The slow changes in the target voltage and the arc current in Fig. 3 were due to slow rise time ($\approx<$ 100 ms) of the power supply used in this experiment. The slow-response power delivers high current at the beginning and much less when the output filter capacitors are discharged. The same gradual change in current and voltage was observed in a previous report, where a slow-response power supply was used and the current peaked and gradually decreased to the set limit current of 2 A [23].

At the initial stage, the target voltage jumped suddenly to -80 V in Fig. 3(b), then fluctuated with the arc current change. Within the 200 μs after the ignition, the voltage settled at around -100 V. This initial jump in the target voltage differed for all arcs and the detail is shown later in Fig. 6(a). For the longer time scale, the arc current and the target voltage changed with an inverse relationship. Similar tendencies have been observed in other researches [16], [23], indicating that the arc current and voltage relationship on an electrically biased target would be characterized by the plasma resistance along the He plasma column, as further discussed later.

Each arc in this research sustained for 1-8 ms. Fig. 4 shows the duration of the arcs with respect to arc mean currents. The arc mean current was derived by averaging each current over its time duration, as typically shown in Fig. 3. The duration of the arcs showed an inverse relationship with the arc mean current. Arcs with 10-20 A of mean current sustained for $\sim$4-8 ms, whereas arcs with higher current of $>$20 A survived shorter for 1-4 ms. This result contradicts the previous result, which showed a linear dependence between the arc duration and the arc current [24]. In [24], there existed some area remaining undamaged even after the arc ignition. However, in this research, almost all the area was eroded as shown in Fig. 2(c). It is known that arc spot can sustain as long as the current does not fall below the minimum current per spot [25]. Therefore, the termination of an arc should be regarded that arc spots could not reach another undamaged surface areas at which a new spot can be easily formed. Considering that the arc spots move faster when the arc current becomes higher [26], it is likely that the number of simultaneous spots increased and the arc spots moved and eroded the surface faster compared to the lower current case, resulting in earlier termination of arc. It has been reported that arc continued for $\sim$15 ms at the arc mean current of 11 A [24]. Therefore, it is possible that the arc duration could be longer if a broader surface area was given in the present research.

B. Arc trail observation

Fig. 5 shows SEM images of a sample surface after the arc ignition. A laser spot, which was introduced to ignite the arcing, is shown in Fig. 5(a). A black dot represents the laser spot center, where the strongest damage occurred, and is surrounded by the rather gray ring-like region, at which arc spots started to ignite. Several arc spots ignited, and some of them survived and spread all over the surface. The inset shows one of arc trails which terminated near the laser spot. The typical spot size was $\sim$5 μm in diameter and multiple stamping on the same position over the previous spots made the whole trail width wider than the individual spot size.

It is noteworthy that there appeared a clean region outside of the laser spot. It looked dark gray by the naked eye, indicating that the surface was damaged but remained a certain fine structure. In this region only several arc trails moved rather linearly toward the outside, as clearly seen in Fig. 5(a). In the

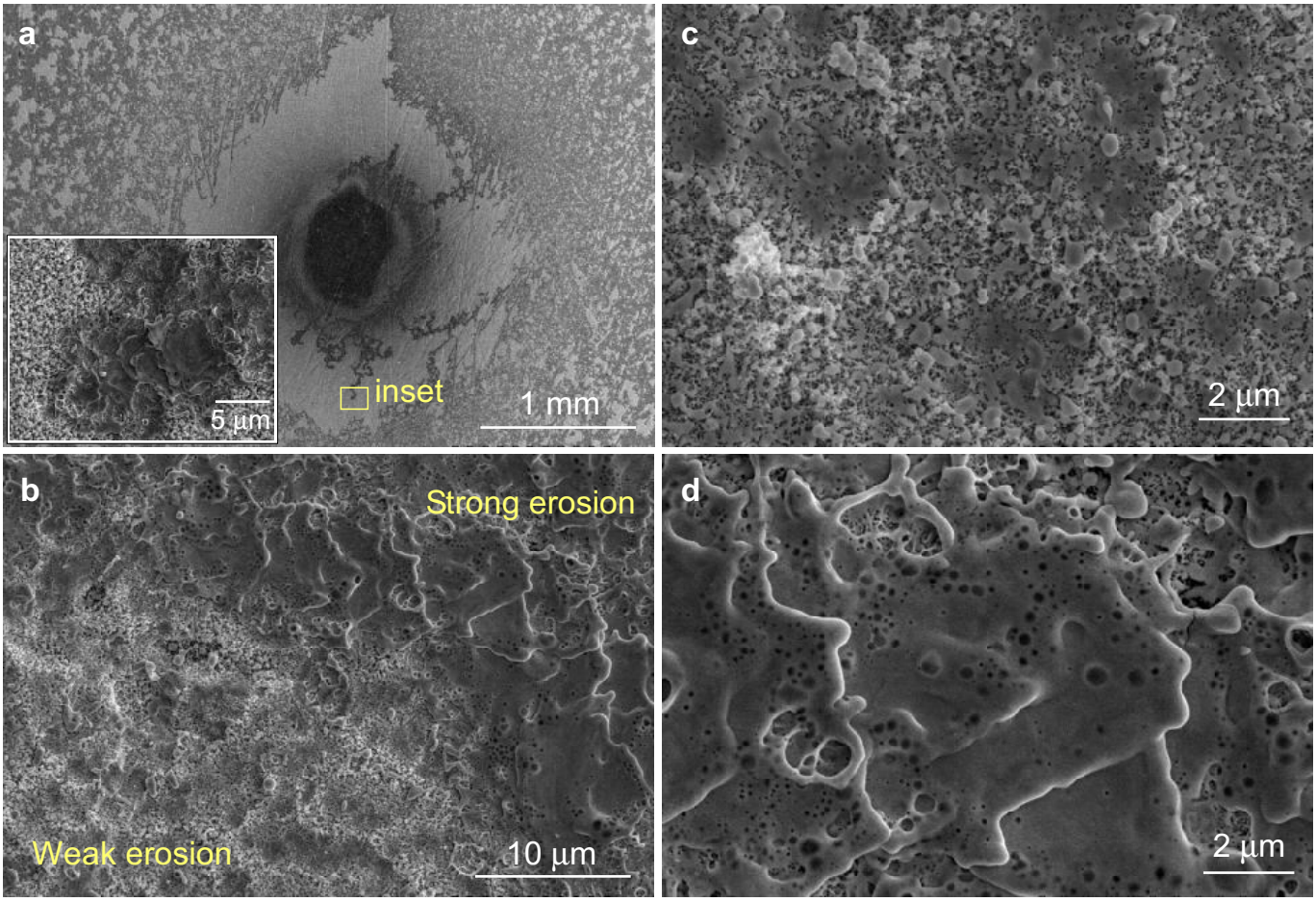

Fig. 5. (a) Laser spot and surrounding arc trails. The inset shows the trail in which arc spots terminated. (b) Two types of typical arc trails, namely weak erosion trail and strong erosion trail, respectively. Enlarged SEM images are shown for (c) weak and (d) strong trails.

inset of Fig. 5(a), the aggregation of nanowires, which is not observed on an original fuzzy surface, is detected on the top of layer that arc spots did not touch. It is probably due to the thermal load by the laser pulse. It was reported that the arc spot velocity was ∼100 m/s at ∼4 A arc [27]. Because the initial arc current in this research was ∼20 times greater compared to the arc current in [27], the arc spot velocity in this research would be much faster. If we assume that the arc spot velocity is ∼500 m/s, the time scale for the arc spots to cross the region would be ∼1 μs, ∼150 times longer than the laser pulse duration of 6 ns. Therefore, it is likely that this region was formed earlier than the arc spots crossing it.

The length of thermal diffusion from a laser spot across the surface is shown as $l \sim \sqrt{\alpha t}$ where α is thermal diffusivity of W. When α ∼40 mm^2/s for W [28], time for the laser pulse load to diffuse across the 0.3-mm-radius gray area in Fig. 5(a) is calculated as ∼2 ms. Therefore, it is more reasonable to think that the deformation in the gray area was due to expansion of laser ablated plasma rather than the thermal diffusion. The degradation of a top layer in the inset of Fig. 5(a) also supports this idea, indicating the thermal load was introduced from the surface, not the substrate.

Because arc spots move in the self-avoiding manner [29], it is likely that the arc spots initiated at the boundary of the laser spot to avoid the severely damaged region and only a few spots could survive. For instance, an aluminum ablation plasma with ambient air of 1 Pa can reach its maximum pressure of 2×10^8 Pa after 15 ns from the initiation, and maintained above $\sim10^5$ Pa in ∼2 mm of radius after 100 ns [30]. It is also likely that a dense tungsten plasma ablated by the laser pulse can sustain and expand for ∼1 μs [31]. Therefore, arc spots could be expelled from the center of laser spot to the outside at the initial state of ignition.

After the initial state of arc ignition, arc spots were broadened all over the surface. Fig. 5(b) shows typical arc trails which were observed in this research. Two distinctive trails, namely weak and strong erosion trails, were distinguished. The entanglement of arc trails, i.e. arc spot grouping, was observed across the whole surface. Typical trail width for the weak trail was ∼5 μm, which was similar to or slightly smaller than the values reported previously [16], [29]. With detailing of the weak trail, as shown in Fig. 5(c), smaller craters were detected. The size of each crater was in the range of 1−4 μm and separated touching the boundaries each other. At the boundary of each crater, damaged fuzzy layer remained and melted droplets formed on it. Porous structure was observed on the bottom of the craters, indicating that fuzzy nanostructures still existed beneath the craters. Fig. 5(d) shows the detailed

image of the strong erosion trail. Nanostructured layer was totally melted out and probably eroded significantly. Different from the weak trail, it seems that each crater overlapped with the former craters. The size of each crater was approximately ∼5-10 μm, which was greater than that of the weak trail. Many dots were detected on the surface of the craters, representing that He bubbles were contained inside the nanowires [32].

From the SEM images of the trails, one can recognize that cathode spots on a fuzz surface fits in the type II classification [33]. On the strong trail in Fig. 5(d), typical craters on a fuzz surface are large in diameter (∼10 μm) with high erosion rate (∼1 mg/C [24]) and adjacent to each other, which are typical properties of the type II spots. It is also known by spectroscopy that an arc on a fuzz surface mostly consists of metal plasmas [23]. On the other hand, there appear several unique properties which are different from the conventional type II spot. The weak trail in Fig. 5(b) shows connections of each spot, though individual spots are separated as shown in Fig. 5(c) with relatively smaller diameter of ∼2 μm. Under the surface of the craters, there still remain fine fuzz structures on the weak trails, implying that the arc ignited touching the upper surface of a fuzzy layer, which is similar to the characteristic of the type I spot occurring on a contaminated layer. In addition, an arc on fuzz easily ignites by adding an additional heat trigger (i.e., laser pulse or plasma pulse) and can sustain even at relatively low current. These properties may due to the lower thermal diffusivity and mass density of fuzz, which requires smaller current density for ignition.

It is still veiled why these two types of spots appear on the same place. Recently, it was suggested that arc spots can sink the same place of a fuzzy layer when the thickness of the fuzzy layer, which is assessed from a cross-sectional SEM image of a fuzzy layer, is thicker than the radius of individual spot cell [34]. In addition, individual spot cells were clearly seen when the fuzz thickness decreased to sub-μm. Thus, it is likely that the strong erosion trail could result from the secondary erosion on the same place where the former arc spots once exploded, allowing the layer to be eroded slightly.

C. Target potential dependence of arc current and voltage

As shown in Fig. 3, the arc current initially peaked and decreased gradually. To understand the influence of bias voltage on the current-voltage characteristic, we focused on the initial and the last 200 μs of the arc pulse, as depicted in Fig. 3. The current and voltage were averaged for each region. Fig. 6(a) shows the dependence of arc voltages at the peak ($V_{\rm peak}$) and the end ($V_{\rm end}$) regions with respect to the initial sheath potential drop ($V_{\rm sh}$), which is the potential drop between the initial target bias and the plasma potential across the sheath region. The corresponding arc currents $I_{\rm peak}$ and $I_{\rm end}$ against $V_{\rm sh}$ are shown in Fig. 6(b).

At the initial stage of the arc, $V_{\rm peak}$ increased linearly as $V_{\rm sh}$ increased, as shown in Fig. 6(a). Correspondingly, $I_{\rm peak}$ linearly decreased and marked the highest current of 100 A when the potential drop was the lowest, -200 V. Considering that the arc current depends on the number of arc spots igniting simultaneously [33], it is likely that a greater potential drop

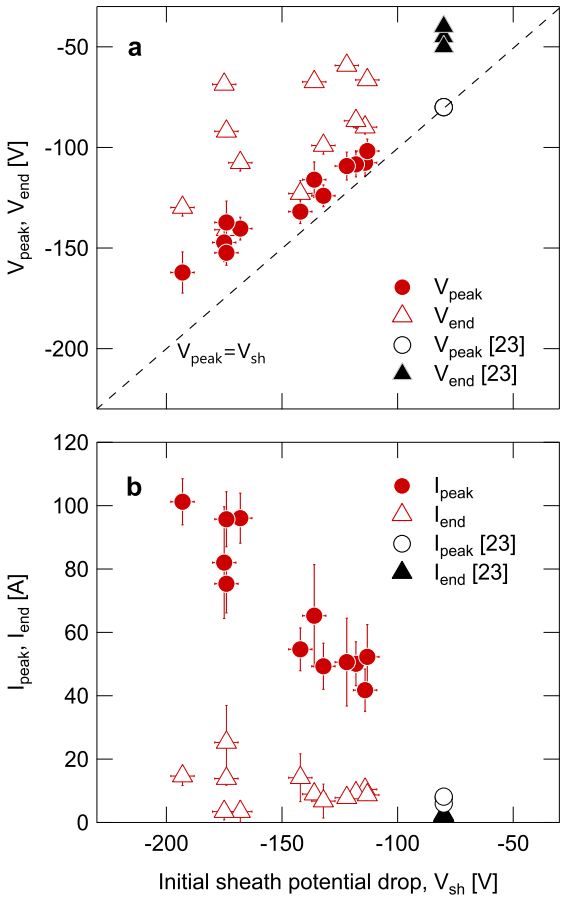

Fig. 6. (a) Arc voltage and (b) arc current of each arc pulse averaged at the first and the last 200 μs with respect to initial sheath potential drop between. Black markers show the results of previous report [23].

between the target and the He plasma results in initiations of a greater number of arc spots and consequently a higher peak current. This can be also conjectured from the previous report [35], where the arc emission area was brightest at the initial stage and gradually decreased as arc progressed when 20-70 A arcs were initiated with similar experimental conditions. This linear dependence is consistent with previous result [23], where ∼8 A-arc ignites at $V_{\rm peak}$ =-80 V, as marked as open circle in Fig. 6.

It is interesting to note that a sudden jump in voltage at the initial stage as typically shown in Fig.3(b) was more remarkable when arc current was higher. At $I_{\rm peak}$ =200 A, the discrepancy between $V_{\rm peak}$ and $V_{\rm sh}$ was ∼30 V, whereas there was no jump in voltage at 8 A arc [23]. The reason of this sudden voltage jump is unclear. One possibility is that an arc plasma formed on the target surface had a size comparable to the target and changed electrical properties instantly. From the fast framing images in [35], an arc plasma column was formed at ∼15 mm toward the axial direction to the target plane and vanished within ∼20 μs then localized near the surface afterward. This result was consistent with the temporal voltage change shown in the peak region of Fig. 3(b), where the target voltage peaked at first then decreased analogously

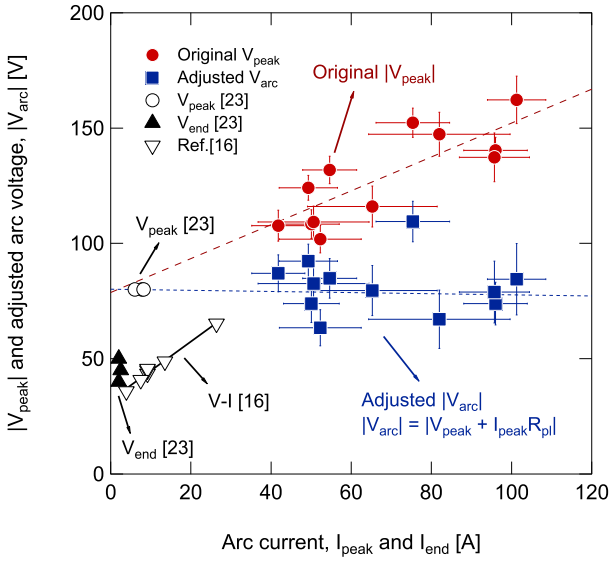

Fig. 7. The relationship between target voltage and arc current measured at the first and the last 200 μs of arc pulses. Red close circles represent the original $|V_{\rm peak}|$ values, whereas blue close rectangles show the adjusted arc current-voltage characteristic where the arc voltage $|V_{arc}|$ was derived by subtracting voltage drop occurring across the He plasma resistance, R_{pl}. Black open circles and close triangles show $|V_{\rm peak}|$ and $|V_{\rm end}|$ values in [23], respectively, and black open triangles show a current-voltage characteristic when a fast-response power supply was used [16].

with arc current change.

In the previous reports, arc burning voltage was considered to be 30-40 V [16], [33]. When a slow-response power supply is used for biasing [23], the voltage at the final stage of an arc ignition, namely end region in Fig. 3, at which the arc current becomes stationary would be close to arc burning voltage.

Triangle markers in Fig. 6 show the target voltage and the arc current at the last 200 μs of discharge, $V_{\rm end}$ and $I_{\rm end}$, respectively. From the previous report [23], $V_{\rm end}$ marked $\sim$-40 V which is close to arc burning voltage for W. On the other hand, $V_{\rm end}$ in the present paper is distributed in the wide range of -60-140 V, which is negatively deeper than typical arc burning voltage. At the moment, this discrepancy is difficult to explain. One possibility is in the fact that arc burning voltage can be affected by external conditions such as He plasma parameters and magnetic field and so on [16], [23]. In the present configurations, He plasma parameters were different for each arc, probably affecting arc burning voltage to be varied. It should also be noted that there exists a possibility that $I_{\rm end}$ in some arc cases with relatively short durations did not reach steady state, indicating that $V_{\rm end}$ could become closer to the arc burning voltage.

D. Current-voltage characteristics via He plasma resistance

It is well known that arc burning voltage is stable at relatively low value: $\sim$30 V for W [33]. Therefore, the linear tendency of $V_{\rm peak}$ in Fig. 6(a) may contain different factor. It has been declared that the current-voltage characteristic of arc can be affected by the plasma resistance formed via the plasma column from a target [16]. Similar to the previous result, the targets in this research were negatively biased and thus it is likely that a global current circuit formed along the He plasma column. Fig. 7 shows the current-voltage characteristics using $I_{\rm peak}$-$V_{\rm peak}$ in Fig. 3 and Fig. 6. Red close markers show the original tendency of $V_{\rm peak}$ with respect to $I_{\rm peak}$. An inversely linear relationship was observed. This tendency was consistent with a previous report [16]. Because it is generally understood that the arc burning voltage is hardly dependent on the arc current [36], this result is probably because of the voltage drop through the He plasma column. The Spitzer resistivity for a single ion species [37] is expressed as

$$\eta = 5.2 \times 10^{-5} \frac{\ln\Lambda}{T_{\rm e}^{3/2}} \quad \Omega \cdot m, \tag{1}$$

where $\ln\Lambda$ is the Coulomb logarithm and $T_{\rm e}$ is the electron temperature of the He plasma in eV. Considering the dimension of emission area of arc spots of $\sim$50 mm^2 with assumption of a symmetric emission area [35] and the length of He plasma of $\sim$1.5 m in the PISCES-A device, the plasma resistance for each plasma can be estimated in the range of 0.6$-$1.1 Ω. Blue rectangle markers in Fig. 7 show the adjusted arc current-voltage characteristics using (1). The arc burning voltage V_{arc} was derived by subtracting the voltage drop by the He plasma resistance from $V_{\rm peak}$. As for V_{arc}, it was estimated to be $\sim$-80 V. The linearly fitted line of $V_{\rm peak}$ also had the same value at the intercept and the slope showed a specific resistance of $\sim$0.8 Ω, which was in a good agreement with the plasma resistances estimated using (1).

The value $|V_{arc}| = 80$ V is $\sim$50 V lower than the arc burning voltage of 30-40 V [33]. As mentioned above, because of the slow response of the power supply, $V_{\rm end}$ would be rather close to the arc burning voltage. However, $V_{\rm end}$ in this research did not show clear linearity. Instead, we can discuss the validity of the current-voltage characteristics by comparing the previous reports. For lower current case [23], $I_{\rm peak}$-$V_{\rm peak}$ characteristics are expressed as black open circles, indicating a good consistence with the results of present research, as shown in Fig. 7. In [23] $V_{\rm end}$ was $\sim$40 V, which was similar to the arc burning voltage. On the other hand, current-voltage characteristics showed an inverse linear relationship, and the adjusted target voltage was more or less the same as the arc burning voltage when a fast-response power supply was used [16]. However, considering that the slope of two cases showed a good agreement and that actual plasma parameters were similar, the evaluation of plasma resistance using the slope of $V_{\rm peak}$-$I_{\rm peak}$ characteristics was valid. Taking into account the discussion above, it is likely that $I_{\rm peak}$-$V_{\rm peak}$ characteristics were affected by He plasma resistance and the actual arc burning voltage would be higher than -80 V. In any case, the linear dependence between the arc current and voltage would be a good feature for fusion devices. It implies that a higher potential drop should be maintained to initiate higher-current arcing, indicating that a high-current arc can be prevented by controlling the potential drop between the plasma and the plasma-facing wall.

E. Ignition and sustainment condition

The arc ignition was controlled by changing the target biasing voltage and the He plasma parameters. Fig. 8(a) shows

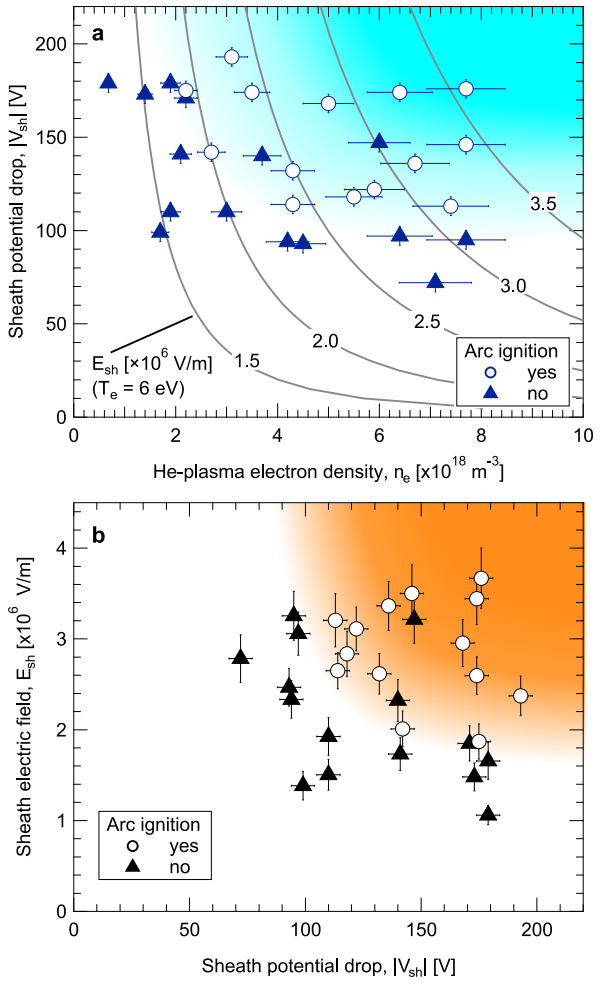

Fig. 8. Arc ignition conditions with varied (a) the sheath potential drop $|V_{sh}|$ and the electron density of He plasma n_e and (b) the sheath electric field E_{sh} and $|V_{sh}|$. Note that the arc ignition regions were colored to guide eyes.

the map of arc ignition, which depended on the potential drop across the sheath between the target and the plasma, $|V_{sh}|$, and the electron density of He plasmas, n_e. Note that the colored region was drawn to guide eyes. The arcs ignited when $|V_{sh}|$>100 V and $n_e > 2 \times 10^{18}$ m^{-3}. When $n_e < 2 \times 10^{18}$ m^{-3}, no arcing initiated even though V_{sh} was greater than 100 V. It is noteworthy that the threshold of $|V_{sh}| > 100$ V for arc ignition in the present study is significantly higher than the previously reported value of $|V_{sh}| > 50 - 60$ V [13], [15]. In [13], $|V_{sh}| > 50$ V was required to initiate 4 A-arc. For higher current, a target required deeper potential because an additional voltage drop occurred across the He plasma resistance in [16], where 65 V was needed for 26 A-arc. When the arc current was ~100 A, even deeper potential drop, say $|V_{sh}| = 100$ V or greater, was necessary to sustain the arc discharge. Therefore, higher threshold voltage required in this research was probably due to greater voltage drop along the He plasma column for high current arcs.

It is known that Child-Law sheath electric field E_{sh} at the surface of a target [38] is expressed as

$$E_{sh} = \frac{4}{3}\frac{V_{sh}}{s} = \frac{1}{\lambda_D}(8T_e^3 V_{sh})^{1/4} = \sqrt{\frac{en_e}{\epsilon_0}}(8V_{sh}T_e)^{1/4} \quad \text{V/m}, \tag{2}$$

where s is the sheath thickness, λ_D is the electron Debye length, e is the elementary electric charge and ϵ_0 is the permittivity of vacuum. The curve lines in Fig. 8(a) show the calculated E_{sh} with an assumption of $T_e = 6$ eV. It is clearly shown that arc did not occur when $|V_{sh}|$ was below 100 V even at the same E_{sh}. The minimum E_{sh} for the arc ignition was $\sim 2 \times 10^6$ V/m.

Fig. 8(b) shows the ignition condition with respect to E_{sh} and $|V_{sh}|$. A clear threshold in E_{sh} existed near ~2 MV/m. At $|V_{sh}| \sim 150$ V, there appear two cases where arcs did not occur even though the experimental condition satisfied the arc ignition criterion. Note that all the arcs in this research ignited at the first trial of laser pulse exposure at each condition. Iterative laser pulse exposures at the same condition would reveal the clearer ignition criterion based on a statistical analysis. This threshold is three orders of magnitude smaller than an electric field of ~10^3 MV/m, which is required for arc ignition on a smooth metallic surface [28], and also an order of magnitude smaller than that of ~15 MV/m for micro-breakdown on W fuzzy layers in vacuum [8]. Considering that the Nd:YAG laser power density is sufficient to ablate the surface and makes dense metallic plasmas, it is likely that the threshold in E_{sh} does not represent an arc ignition condition but a self-sustainment condition.

Without a transient heat load, vacuum breakdown occurred on a typical fuzzy surface at an electric field of ~15 MV/m. It was also featured that the onset of field electron emission started at ~5 MV/m for fuzzy layer [8]. Both values are several times greater than $E_{sh} > 2$ MV/m, which was required for sustainment of arcs in this research. This indicates that the sustainment of arcs is not due to cold field emission but thermo-field emission with heating effect on the vicinity of arc spots. It has been understood that explosive electron emission inducing crater formation requires $10^{10} - 10^{13}$ A/m^2 of current density for bulk metal [39]. However, when an electric field of 2 MV/m is introduced on a smooth W surface of ~4000 K, thermo-field emission gives ~10^9 A/m^2 [40], which is more than one order of magnitude lower than the required current density for the explosive emission. On fuzzy surfaces, the arc spot formation due to the explosive electron emission process [41] would be fueled by two factors. One is the field enhancement effect of nanowires which would enhance the effective electric field strength. The other is the low thermal conductivity of fuzzy layer, which is ~0.6 % or less of bulk W [42]. This would enhance local heating in the vicinity of the exiting arc spots, which enhance the thermo-field emission, and eventually result in formation of new explosive emission spots.

To further understand the ignition properties of the arcs in a surrounding plasma, it would be important to clarify the meaning of the threshold values in a theoretical manner. It is interesting to note that average ohmic electric field at an

explosive plasma $< E >=< j/\sigma >$, where j is current density and σ is the electric conductivity of W, corresponds to the range of 1-10 MV/m [43], which is similar to the electric field threshold for this paper. The ohmic electric field is generated by the presence of cathode fall region, where a voltage drop occurs through the cathode sheath [44]. It is also known that the voltage drop in cathode sheath is needed to maintain a discharge [33]. This comparison gives us a possibility that the existence of electric field threshold in this paper can be generally understood using theoretical description of vacuum arcs. To avoid severe arc ignition in fusion devices, it seems necessary to reduce $n_{\rm e}$ and $T_{\rm e}$, which lowers $V_{\rm sh}$ and $E_{\rm sh}$ in front of the plasma-facing material surface.

IV. Conclusion

In this research, the laser-induced arc was initiated on the tungsten nanostructured 'fuzz' cathode surface which was simultaneously exposed to stationary helium plasmas. Arc ignited right after the pulsed laser irradiation and sustained for several ms. Arc duration was inversely proportional to arc current probably because of greater number and faster movement of arc spots at higher current on limited surface area. An inversely linear arc current-voltage relationship was characterized as a consequence of voltage drop occurring along the helium plasma column. The voltage drop was originated from the resistivity of helium plasma. It was revealed that the ignition and sustainment of arcs were very sensitive to both potential and electric field forming between the target and the plasma. Arcs ignited when the target potential $|{\rm V_{sh}}|$ was larger than 100 V and the sheath electric field $\rm E_{sh}$ was above 2×10^6 V/m, which was 10 times lower than the electric field of $\sim10^7$ V/m for vacuum breakdown on tungsten fuzz layers. The relatively low electric field threshold would result from the thermo-field emission aided by heating of spots from adjacent former spots. Spot explosion and consequent arc ignition at low $\rm E_{sh}$ on fuzzy layer was discussed, raising possibilities of field enhancement effect by the elongated morphology of nanowires and significantly degraded thermal conductivity of fuzzy layer. It was conjectured that a greater potential gap should be maintained to keep a higher arc current, which shows a good sign for preventing a high current arc in fusion devices.

Acknowledgment

This work was supported in part by JSPS KAKENHI 15H04229, 17J05670 and JSPS Bilateral Joint Research Projects. This work was supported in part by LGS frontier program of Nagoya University by JSPS. This work was supported in part by the U.S. Department of Energy Grant No. DE-FG02-07ER54912. This work was supported in part by RFBR Grants 18-58-50005, 16-08-01306 and by the RAS Presidium (basic research programme I.11P).

References

[1] G. Federici, A. Loarte, and G. Strohmayer, "Assessment of erosion of the ITER divertor targets during type I ELMs," Plasma Phys. Control. Fusion, vol. 45, pp. 1523, 2003.

[2] S. Takamura, N. Ohno, D. Nishijima, and S. Kajita, "Formation of nanostructured tungsten with arborescent shape due to helium plasma irradiation," Plasma and Fusion Research: Rapid Communications, vol. 1, pp. 051, 2006.

[3] M. J. Baldwin and R. P. Doerner, "Helium induced nanoscopic morphology on tungsten under fusion relevant plasma conditions," Nucl. Fusion, vol. 48, pp. 035001, 2008.

[4] S. Kajita, W. Sakaguchi, N. Ohno, N. Yoshida, and T. Saeki, "Formation process of tungsten nanostructure by the exposure to helium plasma under fusion relevant plasma conditions," Nucl. Fusion, vol. 49, pp. 095005, 2009.

[5] R. A. Pitts, S. Carpentier, F. Escourbiac, T. Hirai, V. Komarov et al., "A full tungsten divertor for ITER: Physics issues and design status," J. Nucl. Mater., vol. 438, pp. S48-S56, 2013.

[6] G. De Temmerman, T. Hirai, and R. A. Pitts, "The influence of plasma-surface interaction on the performance of tungsten at the ITER divertor vertical targets," Plasma Physics and Controlled Fusion, vol. 60, no. 4, p. 044018, Apr. 2018.

[7] S. Kajita, T. Yagi, K. Kobayashi, T. Masayuki, and N. Ohno, "Measurement of heat diffusion across fuzzy tungsten layer," Results in Phys., vol. 6, pp. 877-878, 2016.

[8] D. Hwangbo, S. Kajita, N. Ohno, and D. Sinelnikov, "Field emission from metal surfaces irradiated with helium plasmas," IEEE Trans. Plasma Sci., vol. 45, pp. 2080–2086, 2017.

[9] D. L. Rudakov, C. P. C. Wong, R. P. Doerner, G. M. Wright, T. Abrams et al., "Exposures of tungsten nanostructures to divertor plasmas in DIII-D," Phys. Scr., vol. T167, pp. 014055, 2016.

[10] S. Kajita, M. Fukumoto, M. Tokitani, T. Nakano, Y. Noiri et al., "Impact of arcing on carbon and tungsten: from the observations in JT-60U, LHD and NAGDIS-II," Nucl. Fusion, vol. 53, pp. 053013, 2013.

[11] M. Tokitani, S. Kajita, S. Masuzaki, Y. Hirahata, N. Ohno, T. Tanabe, and LHD Experiment Group, "Exfoliation of the tungsten fibreform nanostructure by unipolar arcing in the LHD divertor plasma," Nucl. Fusion, vol. 51, pp. 102001, 2011.

[12] V. Rohde, M. Balden, N. Endstrasser, U. von Toussaint, and ASDEX Upgrade team, "Tungsten erosion by arcs in ASDEX upgrade," J. Nucl. Mater., vol. 438, pp. S800, 2013.

[13] S. Kajita, N. Ohno, N. Yoshida, R. Yoshihara, and S. Takamura, "Arcing on tungsten subjected to helium and transients: ignition conditions and erosion rates," Plasma Phys. Control. Fusion, vol. 54, pp. 035009, 2012.

[14] S. Kajita, S. Takamura, and N. Ohno, "Prompt ignition of a unipolar arc on helium irradiated tungsten," Nucl. Fusion, vol. 49, pp. 032002, 2009.

[15] M. Yajima, N. Ohno, S. Kajita, G. De Temmerman, K. Bystrov, S. Bardin, T. W. Morgan, and S. Masuzaki, "Investigation of arcing on fiber-formed nanostructured tungsten by pulsed plasma during steady state plasma irradiation," Fusion Eng. Des., vol. 112, pp. 156-161, 2016.

[16] D. Hwangbo, S. Kajita, S. A. Barengolts, M. M. Tsventoukh, S. Kawaguchi, V. G. Mesyats, and N. Ohno, "Ignition and erosion of materials by arcing in fusion-relevant conditions," Contrib. Plasma Phys., vol. 58, pp. 608-615, 2018.

[17] D. U. B. Aussems, D. Nishijima, C. Brandt, H. J. van der Meiden, M. Vilémová et al., "The occurrence and damage of unipolar arcing on fuzzy tungsten," J. Nucl. Mater., vol. 463, pp. 303-307, 2015.

[18] D. M. Goebel, G. Campbell, and R. W. Conn, "Plasma surface interaction experimental facility (PISCES) for materials and edge physics studies," J. Nucl. Mater., vol. 121, pp. 277-282, 1984.

[19] T. J. Petty, M. J. Baldwin, M. I. Hasan, R. P. Doerner, and J. W. Bradley, "Tungsten 'fuzz' growth re-examined: the dependence on ion fluence in non-erosive and erosive helium plasma," Nucl. Fusion, vol. 55, pp. 093033, 2015.

[20] N. Vogel and H. Höft, "Cathode spot energy transfer simulated by a focused laser beam," IEEE Trans. Plasma Sci., vol. 17, pp. 638-640, 1989.

[21] S. A. Barengolts, G. A. Mesyats, and M. M. Tsventoukh, "Initiation of ecton processes by interaction of a plasma with a microprotrusion on a metal surface," J. Exp. Theor. Phys., vol. 107, no. 6, pp. 1039-1048, Dec. 2008.

[22] S. A. Barengolts, G. A. Mesyats, and M. M. Tsventoukh, "Explosive Electron Emission Ignition at the "W-Fuzz" Surface Under Plasma Power Load," IEEE Trans. Plasma Sci., vol. 39, no. 9, pp. 1900-1904, Sep. 2011.

[23] D. Hwangbo, S. Kajita, M. Osaka, and N. Ohno, "Spectroscopic Study and Motion Analysis of Arc Spot Initiated on Nanostructured Tungsten," Japanese Journal of Applied Physics, vol. 52, no. 11S, p. 11NC02, 2013.

[24] D. Hwangbo, S. Kawaguchi, S. Kajita, and N. Ohno, "Erosion of nanostructured tungsten by laser ablation, sputtering and arcing," Nucl. Mater. Energy, vol.12, pp.386-391, 2017.
[25] I. G. Kesaev, "Cathode Processes in the Mercury Arc," Consultants bureau, New York, 1965.
[26] C. J. Gallagher, "The Retrograde Motion of the Arc Cathode Spot," J. Appl. Phys., vol. 21, pp. 768, 1950.
[27] D. Hwangbo, S. Kajita, S. A. Barengolts, M. M. Tsventoukh, and N. Ohno, "Transition in velocity and grouping of arc spot on different nanostructured tungsten electrodes," Results in Physics, vol. 4, pp. 33-39, 2014.
[28] G. A. Mesyats, "Cathode Phenomena in a Vacuum Discharge," NAUKA, Moscow, 2000.
[29] S. Kajita, N. Ohno, S. Takamura, and Y. Tsuji, "Direct observation of cathode spot grouping using nanostructured electrode," Phys. Lett. A, vol. 373 pp. 4273-4277, 2009.
[30] T. Mocicki, J. Hoffman, and Z. Szymaski, "Modelling of plasma formation during nanosecond laser ablation," Archives of Mechanics, vol. 63, no. 2, pp. 99-116, Warszawa 2011
[31] R. E. Russo, "Laser-Induced Breakdown Spectroscopy," Lawrence Berkeley National Laboratory, 2007.
[32] S. Kajita, N. Yoshida, N. Ohno, and Y. Tsuji, "Growth of multifractal tungsten nanostructure by He bubble induced directional swelling," New J. Phys., vol. 4, pp. 043038, 2015.
[33] A. Anders, "Cathodic Arcs: From Fractal Spots to Energetic Condensation," Springer, NY, 2008.
[34] S. A. Barengolts, V. G. Mesyats, M. M. Tsventoukh, S. Kajita, D. Hwangbo, and N. Ohno, "Effect of the Nanostructured Layer Thickness on the Dynamics of Cathode Spots on Tungsten," IEEE Trans. Plasma Sci., vol. 46, pp. 4044-4050, 2018.
[35] D. U. B. Aussems, D. Nishijima, C. Brandt, R. P. Doerner, and N. J. L. Cardozo, "Spectroscopic characterization and imaging of laser- and unipolar arc-induced plasmas," J. Appl. Phys., vol. 116, pp. 063301, 2014.
[36] W. D. Davis and H. C. Miller, "Analysis of the Electrode Products Emitted by dc Arcs in a Vacuum Ambient," J. Appl. Phys., vol. 40, pp. 2212, 1969.
[37] I. I. Hutchinson, Principles of Plasma Diagnostics, Cambridge University Press, New York, 2002.
[38] M. A. Lieberman and A. J. Lichtenberg, "Principles of Plasma Discharges and Materials Processing," John Wiley & Sons, Inc., NJ, USA, 2005.
[39] G. A. Mesyats, "Ecton Mechanism of the Cathode Spot Phenomena in a Vacuum Arc," IEEE Trans. Plasma Sci., vol. 41, no. 4, pp. 676-694, 2013.
[40] S. Kajita, N. Ohno, Y. Hirahata, and M. Hiramatsu, "Field emission property of nanostructured tungsten formed by helium plasma irradiation," Fusion Engineering and Design, vol. 88, no. 11, pp. 2842-2847, Nov. 2013.
[41] S. A. Barengolts, G. A. Mesyats, and M. M. Tsventoukh, "The ecton mechanism of unipolar arcing in magnetic confinement fusion devices," Nucl. Fusion, vol. 50, pp. 125004, 2010.
[42] S. Kajita, T. Yagi, K. Kobayashi, M. Tokitani, and N. Ohno, Measurement of heat diffusion across fuzzy tungsten layer, Results in Physics, vol. 6, pp. 877-878, 2016.
[43] M. M. Tsventoukh, "Plasma parameters of the cathode spot explosive electron emission cell obtained from the model of liquid-metal jet tearing and electrical explosion," Physics of Plasmas, vol. 25, no. 5, pp. 053504, May 2018.
[44] D. L. Shmelev, S. A. Barengolts, and M. M. Tsventoukh, "Numerical Simulation of Plasma Near the Cathode Spot of Vacuum Arc," IEEE Trans. Plasma Sci., vol. 45, no. 11, pp. 3046-3053, Nov. 2017.

Dogyun Hwangbo was born in Gyeongju, South Korea, in 1989. He received the bachelors degree from the Department of Engineering, Nagoya University, Japan, in 2013, where he is currently pursuing doctoral degree with the Graduate School of Engineering.

His current research interests include plasma surface interaction phenomena, especially arcing, breakdown phenomena, and electron emission process on the nanostructured metallic surfaces.

PLACE PHOTO HERE

Daisuke Nishijima

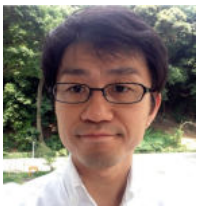

Shin Kajita was born in Nagoya, Japan, in 1977. He received the Dr.Eng. degree from the University of Tokyo, Tokyo, Japan, in 2005.

He is currently an Associate Professor with the Institute of Materials and Systems for Sustain- ability, Nagoya University, Nagoya. His current research interests include plasma-surface interaction phenomena occurred in divertor region and metallic nanostructures formed by the helium plasma irradiation.

Russell P. Doerner received degrees from Texas A&M University (B.S. in Physics, 1981) and the University of Wisconsin-Madison (M.S. in Materials Science, 1984 and Ph.D. in Electrical Engineering, 1988). Since that time he has performed experiments in the edge and scrape-off layer plasma of confinement machines throughout the world and has been involved in fundamental plasma-material interaction measurements conducted in various linear plasma devices. He has worked extensively with the IAEA in numerous plasma-material interactions coordinated research projects and presently leads the plasma-material interaction research program in the PISCES Laboratory at UCSD, and the US-EU Bilateral Collaboration on Mixed-Material Research for ITER.

Sergey A. Barengolts was born in Semipalatinsk, Kazakhstan, Russia, in 1964. He received the High School Diploma degree from Tomsk State University, Tomsk, Russia, in 1986, the Cand.Sci. degree from the High Current Electronics Institute, Tomsk, in 1989, and the Dr.Sci. degree in physics and mathematics from the Institute of Electrophysics Institute, Ekaterinburg, Russia, in 2005.

He is currently the Head of the Electrophysics Research Laboratory, Prokhorov General Physics Institute, Russian Academy of Sciences, Moscow, Russia. His current research interests include vacuum and gas discharges and high-current field emission.

Mikahil M. Tsventoukh was born in Moscow, Russia, in 1982. He received the High School Diploma and Ph.D. degrees from the Moscow Engineering and Physics Institute, State University, Moscow, Russia, in 2005 and 2009, respectively.

From 2015 to 2016, he was a Former Scientific Academic Secretary with the Lebedev Physical Institute, Russian Academy of Sciences, where he is currently a Senior Scientific Researcher. His current research interests include plasma physics, magnetic confinement, numerical modeling, vacuum and gas discharges, and emission processes in plasma-surface interactions.

Noriyasu Ohno was born in 1962 in Japan. He received the Doctor of Science degree from Kyushu University in 1993. Since 2007, he is a Professor of Graduate School of Engineering at Nagoya University. He has been authored and co-authored of more than 300 peer reviewed journals and conference proceedings. He is interested in edge plasma physics in magnetically confined fusion devices, such as plasma detachment associated with atomic and molecular processes, and convective plasma transport, and plasma-material interactions. He is a member of the Fusion Technical Committee in the Ministry of Education, Culture, Sports, Science and Technology in Japan.

Hirohiko Tanaka Hirohiko Tanaka was born in Gifu, Japan in 1986. He received the Dr.Eng. Degree from Nagoya University, Nagoya, Japan, in 2011.

From 2011 to 2016, he was an Assistant Professor with the National Institute for Fusion Science, Gifu. He is currently an Assistant Professor with the Nagoya University. His current research interests include plasma detachment and convective plasma transport in various magnetic confinement fusion devices.